PROCEEDINGS OF SPIE

SPIEDigitalLibrary.org/conference-proceedings-of-spie

Deformable lens for testing the performance of focal plane wavefront sensing using phase diversity

Gabriele Umbriaco, Daniele Vassallo, Jacopo Farinato, Luca Marafatto, Elena Carolo, et al.

Gabriele Umbriaco, Daniele Vassallo, Jacopo Farinato, Luca Marafatto, Elena Carolo, Maria Bergomi, Valentina Viotto, Simone Di Filippo, Stefano Bonora, Jacopo Mocci, Roberto Ragazzoni, Thierry Fusco, Jean-Francois Sauvage, "Deformable lens for testing the performance of focal plane wavefront sensing using phase diversity," Proc. SPIE 12185, Adaptive Optics Systems VIII, 121856W (29 August 2022); doi: 10.1117/12.2629385

SPIE.

Event: SPIE Astronomical Telescopes + Instrumentation, 2022, Montréal, Québec, Canada

Deformable lens for testing the performance of focal plane wavefront sensing using phase diversity

Gabriele Umbriaco[a,b,c], Daniele Vassallo[a,c], Jacopo Farinato[a,c], Luca Marafatto[a,c], Elena Carolo[a,c], Maria Bergomi[a,c], Valentina Viotto[a,c], Simone Di Filippo[a,b,c], Stefano Bonora[d], Jacopo Mocci[e], Roberto Ragazzoni[a,c], Thierry Fusco[f,g], Jean-Francois Sauvage[f,g]

a - INAF Osservatorio Astronomico di Padova, Vicolo dell'Osservatorio 5, 35122 Padua, Italy
b – University of Padova, Dept. Physics and Astronomy, Vicolo dell'Osservatorio 3, 35122 Padua, Italy
c - ADONI - National Laboratory for Adaptive Optics, Italy
d - CNR-IFN, via Trasea 7, 35131, Padova, Italy
e - Dynamic Optics srl, Piazza Zanellato 5, 35131, Padova, Italy
f - Aix Marseille Univ, CNRS, CNES, LAM, Marseille, France
g - DOTA, ONERA, Université Paris Saclay, F-91123 Palaiseau, France

ABSTRACT

SHARK-NIR is a high-contrast camera for the LBT, it has been conceived and designed to fully exploit the high Strehl ratio adaptive optics correction delivered by the FLAO module, which is being upgraded to SOUL, and will implement different coronagraphic techniques, with contrast as high as 10^{-6} down to 5 mas from the star. To maximize the achievable contrast, SHARK-NIR implements a couple of peculiar features, namely a fast internal TT loop to minimize the residual jitter and a local non-common path aberration correction, applied through an internal deformable mirror.
To derive instrumental aberrations, one option is to use the phase diversity technique, which allows wavefront sensing by using two images in intrafocus and extrafocus positions. To calibrate this sensor, we initially assembled a dedicated optical bench equipped with a deformable mirror and a fast IR camera. To characterize phase diversity under more general conditions and independently from the SHARK-NIR setup, we focused then on a new simple test bench, implementing a new (multi-actuator) deformable lens able to reproduce low order aberrations up to 4th order of Zernike polynomials, as an aberration generator. The optical design is simpler and cheaper than using a deformable mirror, which requires a folded optical path and more optics. In this case we used an interferometer to characterize the linearity of the aberration generator and the phase diversity is used for sensing non-common path aberrations (NCPA) in SHARK-NIR.

Keywords: deformable lens, phase diversity, SHARK-NIR, wavefront sensing, wavefront correction

1. INTRODUCTION

Phase diversity [1] (PD) is a focal plane wavefront sensing technique that allows to retrieve the phase aberration introduced by a camera starting from two images of whatever object, one of which (the diverse image) is intentionally corrupted by a known aberration. This technique is used for sensing non-common path aberrations (NCPA) in SHARK-NIR[2], the new-generation high-contrast imager for the Large Binocular Telescope (LBT), now in pre-commissioning phase[3 4].

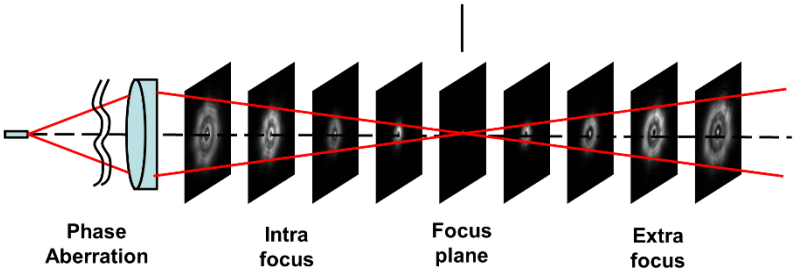

Figure 1 Phase diversity use a set of intra and extra focus images. Here are the images of the set without aberrations.

Adaptive Optics Systems VIII, edited by Laura Schreiber, Dirk Schmidt, Elise Vernet,
Proc. of SPIE Vol. 12185, 121856W · © 2022 SPIE
0277-786X · doi: 10.1117/12.2629385

Phase diversity uses a set of intra- and extra-focus images, as show in the schema of Figure 1. To test the phase diversity, we mount a dedicated test bench composed of: an interferometer to test the correct aberration introduced by the deformable lens, a flat reference mirror for the double pass interferometric test, a lens to introduce known aberrations along the optical path, and a Shack-Hartmann test bench to characterize the reference flat of the lens. Images collected before and after the focus are pre-reduced and used to perform Phase Diversity[5].

2. DEFORMABLE LENS

The deformable lens (AOL1816, Dynamic Optics srl) used in this work is composed by two thin flexible glass membranes (200um thick). The lens has a clear aperture of 16mm, with a diameter of 61mm, the actuators show a response time below 2.5ms and is capable of these amount of aberrations (specification sheet) listed in Table 1. The transmission curve of the deformable lens allows for work from 400nm to 1200nm, see Figure 2. The space between the membranes is filled with a transparent gel. Each of the glass membranes is bonded to a piezoelectric actuator with a ring shape. Each ring is divided into nine independent segments for a total of 18 actuators. Each actuator can be driven independently with a voltage range of +/-125V [6]. The deformable lens can generate aberrations up to the fourth order of the Zernike polynomial with a response time of about 2ms. This type of wavefront corrector has been successfully used in different applications, including astronomical instruments [7] [8]. The picture below shows the response function of each single actuator Figure 3, and the amplitude of the Zernikes mode Figure 4.

Table 1 Zernike polynomials in closed loop (16mm aperture lens, 1wave=0.633nm)

Aberrations	Peak to Valley (waves@633nm)	rms (waves@633nm
Tip	33.0	9.0
Tilt	32.5	9.0
Vertical Astigmatism	19.0	4.0
Defocus	12.0	3.0
Oblique Astigmatism	16.0	3.8
Vertical Trefoil	11.0	1.7
Vertical Coma	5.0	0.8
Horizontal Coma	4.5	1.0
Oblique Trefoil	7.0	1.5
Vertical Quadrifoil	6.8	0.7
Vertical Secondary Astigmatism	3.1	0.3
Horizontal Secondary Astigmatism	3.1	0.3
Oblique Quadrifoil	6.3	0.6
Primary Spherical	1.0	0.2

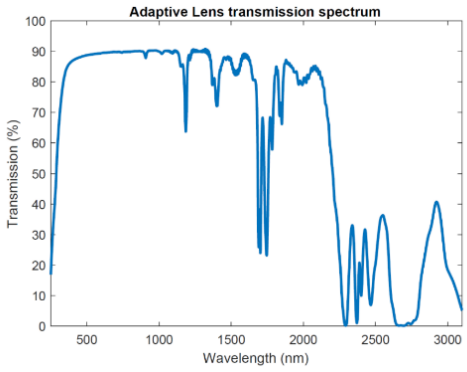

Figure 2 Transmission spectrum of the adaptive lens

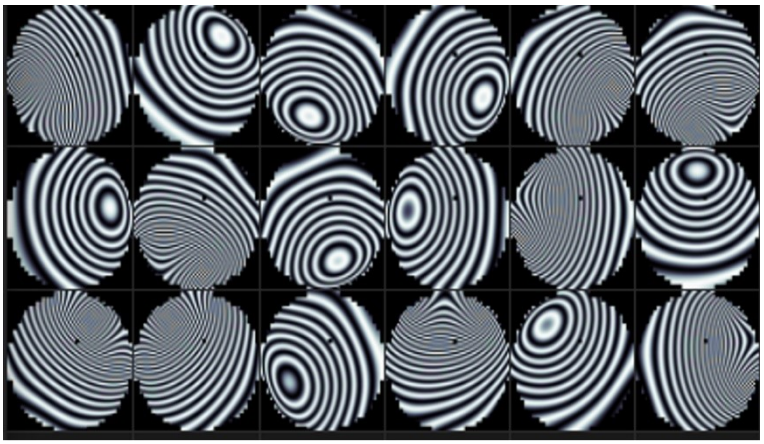

Figure 3 Response function of deformable lens actuators (interferograms @633nm)

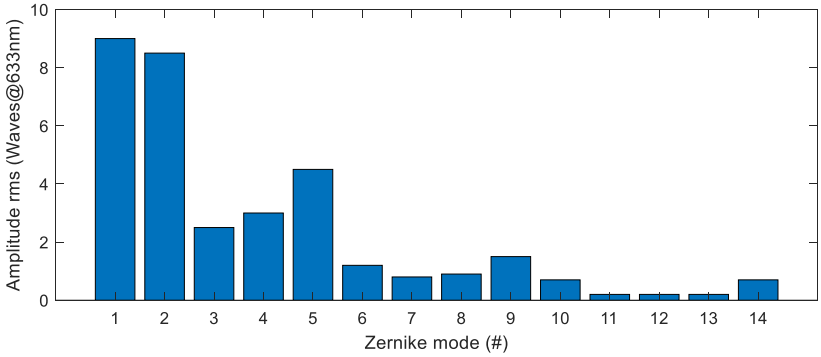

Figure 4 Zernike modes of the deformable lens.

To characterize the response of the deformable lens, we applied to the deformable lens variable aberrations, from -0,12 to 0,12 waves @633nm corresponding to ±76 nm maximum with 6 nm steps. For each step, we measure with the interferometer the amount of aberrations. Figure 5 to Figure 9 show, for each aberration, the amplitude of the response of the lens along the value of aberration pushed.

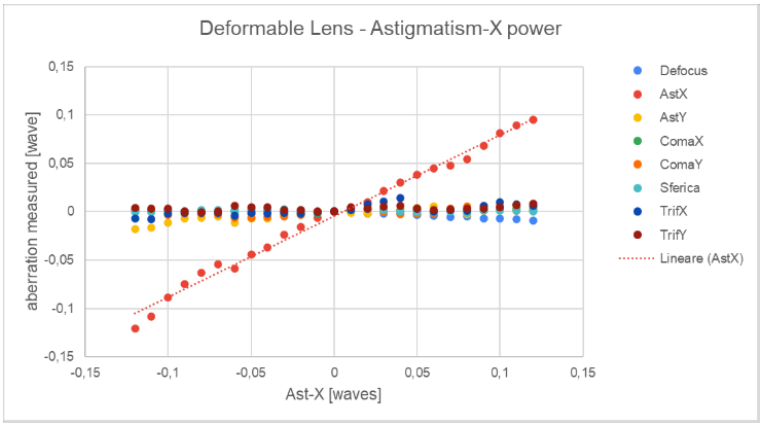

Figure 5 Response of the deformable lens to change in astigmatism X aberration

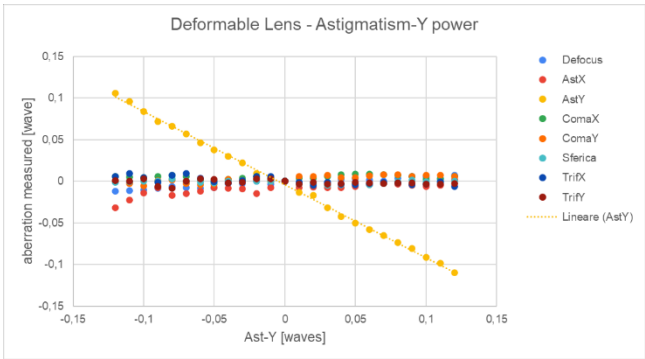

Figure 6 Response of the deformable lens to change in astigmatism Y aberration

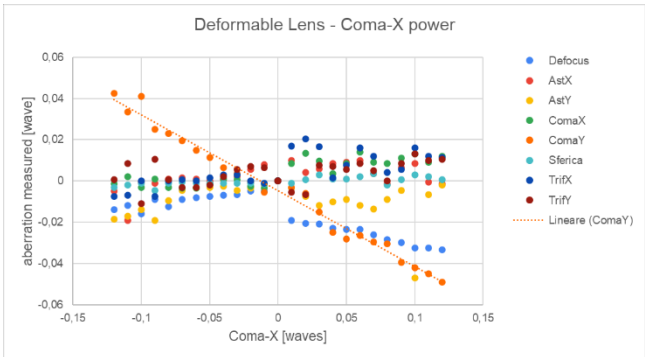

Figure 7 Response of the deformable lens to change in coma X aberration

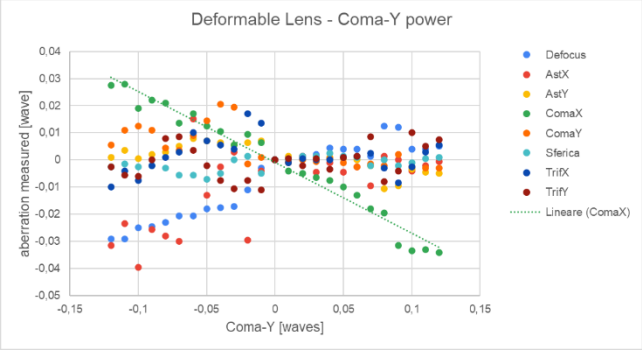

Figure 8 Response of the deformable lens to change in coma Y aberration

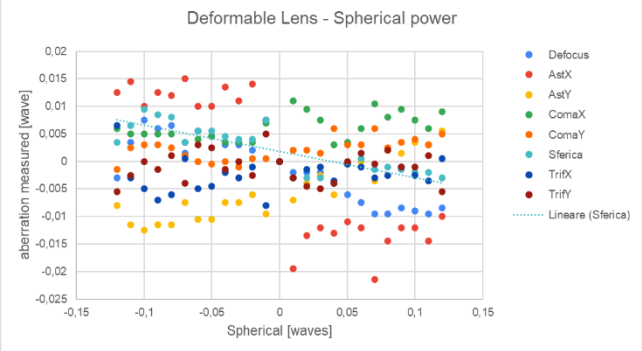

Figure 9 Response of the deformable lens to change in spherical aberration

3. TEST BENCH

To test the phase diversity we mount a dedicated test bench, see schema in Figure 10 and image of the bench in Figure 11, composed of (1) interferometer to test the correct aberration introduced by the (2) deformable lens, (3) folding mirror on translation stage introduced for illuminate the phase diversity arm, (4) flat mirror for the double pass interferometric test, (5) lens to create images aberrated on the CCD mounted on a translation stage. The ccd camera acquires images at a 16bit dynamic range with a pixel of 2,4 microns. The focusing lens with focal of 250mm at 633nm is set to F/# of 15.6. Each set of images was acquired with a stack of 10 images, subtracted by a dark image. The images are then coaligned, using a Gaussian fit for images near the focus and the Fast Library for Approximate Nearest Neighbors (FLANN) [9] for defocused images. The CCD was moved to different positions corresponding to a defocus of 1, 1.5, 2 e 2.5 lambda PtV. The images were acquired with the CCD moving to intra- and extra-focus positions of 0.0. +1.233. +1.849. +2.464. +3.082. -1.233. -1.849. -2.464. -3.082.

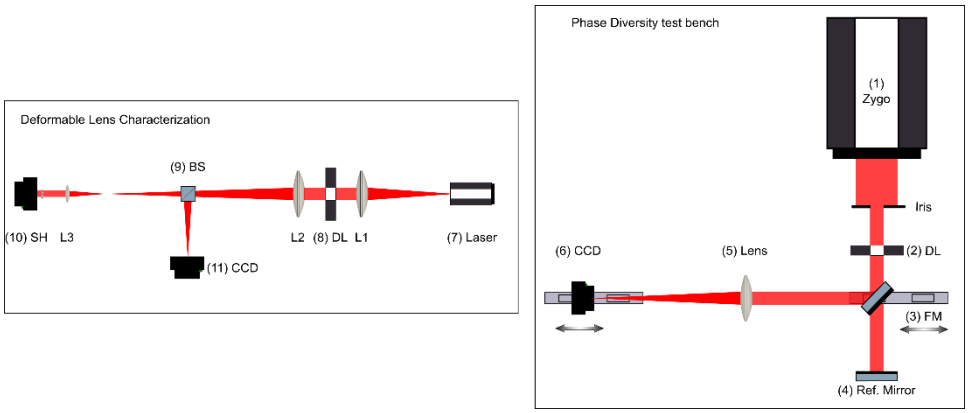

Figure 10 Diagram of the test bench. Left Shack-Hartmann bench to characterize the deformable lens. Right-hand setup to perform the phase diversity.

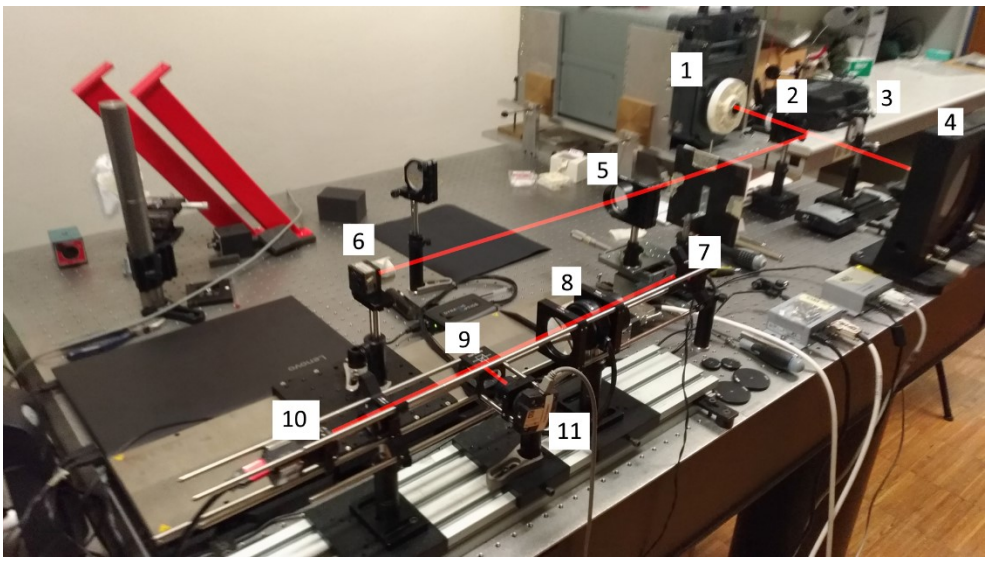

Figure 11 Image of the two sets of devices installed on the same optical bench.

A second Shack-Hartmann test bench, controlled in closed loop, was used to characterize the reference flat of the deformable lens. It is composed of (7) laser source, (8) deformable lens, (9) beam splitter, (10) Shak-Hartmann wave sensor, (11) PSF camera. Two lenses, L1 and L2, are used to put the deformable lens in a collimated beam, refocused to observe the PSF or perform close-loop wave front correction. With the proprietary software of the deformable lens, we place the actuator to minimize the aberration of the lens. In Figure 12 an interferogram of the lens near a flat surface is shown, in this case 0,018 waves (11 nm) RMS. We move the lens in front of the interferometer and start aberration

generation by checking with the interferometer the corresponding amount of aberrations used. By inserting the folding mirror (3) we collect intra- and extra images used for phase diversity.

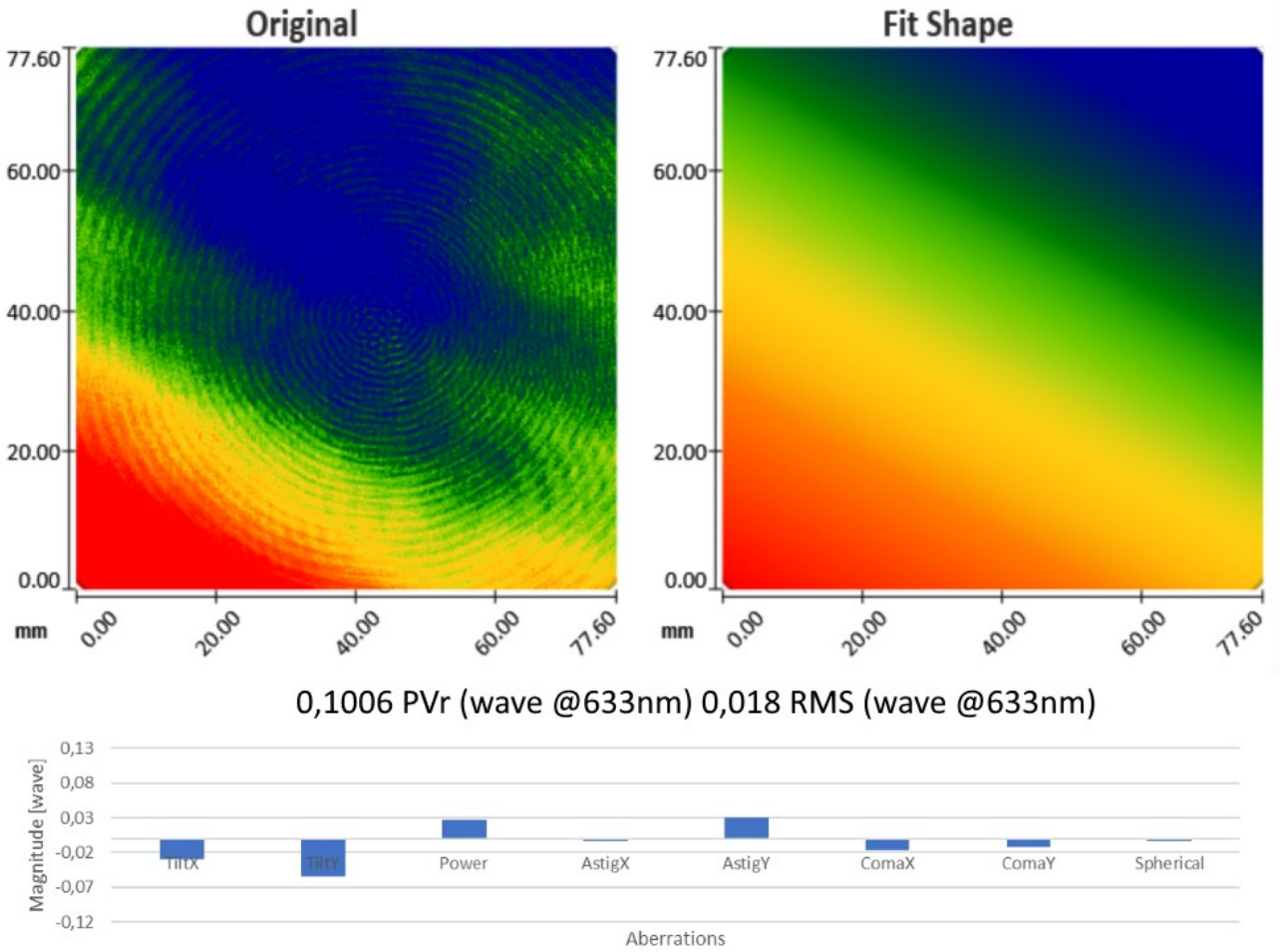

Figure 12 Interferogram of the deformable lens in the positions of reference flat.

On SHARK-NIR the phase diversity is performed using two different fiber optics [9], one used to generate a reference spot, and the other positioned out of focus in the scientific camera. To simulate the defocused fiber, we use the image that corresponds to +1.233mm on defocus. In the final setup of SHARK, two different lenses, with opposite power but same focal length, which allow for 6 different combinations of images in intra- and extra-focus are presented.
We push the lens over astigmatism, coma, and spherical aberration, from -0.12 to 0,12 waves at 633nm (± 76 nm). The set of 9 acquired images is subtracted by dark, and we compute phase diversity above all possible combinations of two or more images, 502 combinations in total.

4. PHASE DIVERSITY

Phase diversity[10] is based on the simultaneous recording of two or more quasi-monochromatic images. In the first image, it is recorded in the focal plane of the optical system. The second image is recorded in an out-of-focus plane.
The distance between these two planes is calibrated and corresponds to a small defocus. The relation between the image and the aberrated phase is nonlinear: no analytical solution exists to derive the latter from the former. The phase can thus be estimated iteratively by minimizing a given criterion. In this work we adopted an optimized method based on a

maximum a posteriori (MAP) approach. This method basically consists of maximizing the likelihood of the data once a theoretical model for the data themselves is chosen.

All images are collected and analyzed using a dedicated Python code. We present a selection of intrafocal and extrafocal plane images with the camera at 3.082mm (2.5 lambda in defocus), corresponding to the maximum amount of astigmatism (Figure 13) and Coma and spherical aberrations (Figure 14).

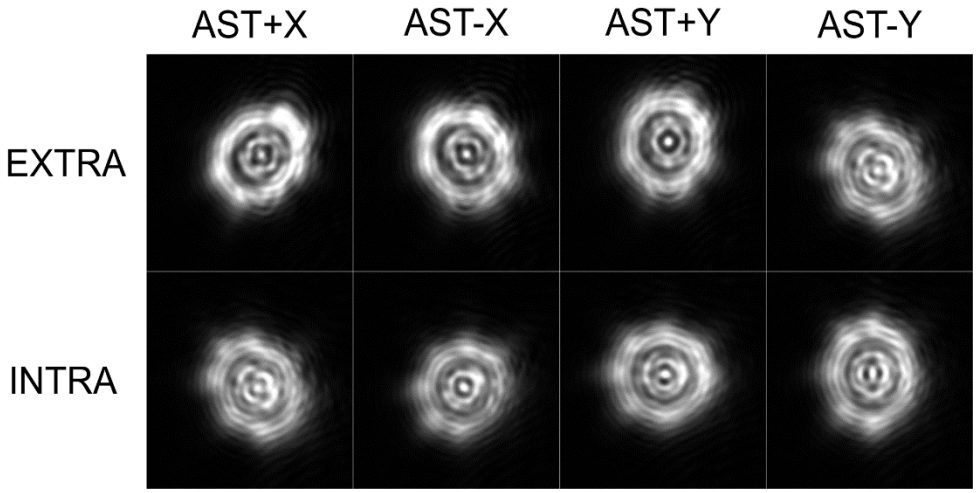

Figure 13 Images intra- and extra-focus of 3.082mm applying two different values, positive and negative same absolute values, for astigmatism X and Y aberrations.

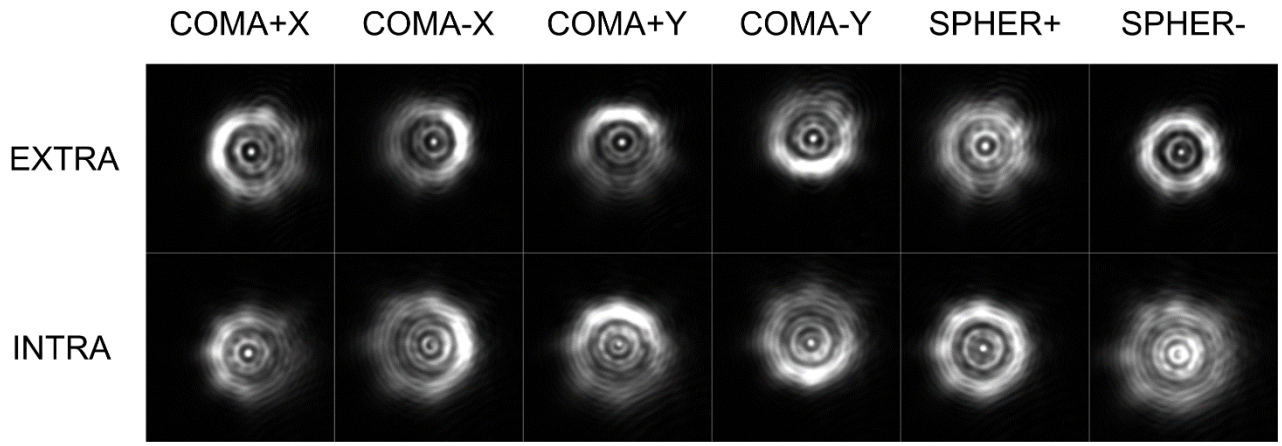

Figure 14 Images intrafocus and extrafocus of 3.082mm applying two different values, positive and negative, the same absolute values, for coma X and Y and spherical aberrations.

Phase Diversity sensing was developed[5] using IDL and the entire dataset counts more than 3000 raw images. In Figure 15 the comparison between Phase Diversity using all 9 images (PD-9) and Zygo interferometer for each single mode aberration injected with DL. Zygo data points are the average of the two interferograms. The flat DL (top panel) shows a 20nm overall discrepancy (mainly coma), which can be attributed to NCPA between the two sensing channels. To eliminate this contribution, we subtracted the respective flats from all of the measurements. In this way, the PD reconstructions match quite well with the Zygo measurements and individual aberrations are well recovered. The only notable discrepancies are in the defocus term. Defocus discrepancies are due to the fact that radial modes suffer from higher reconstruction uncertainties. Moreover, by looking at the interferograms, we noticed that the DL drifts in focus up to 40nm in the worst cases. Such a drift across the PD data set surely affects the reliability of the defocus estimation. No other mode exhibits significant drifts.

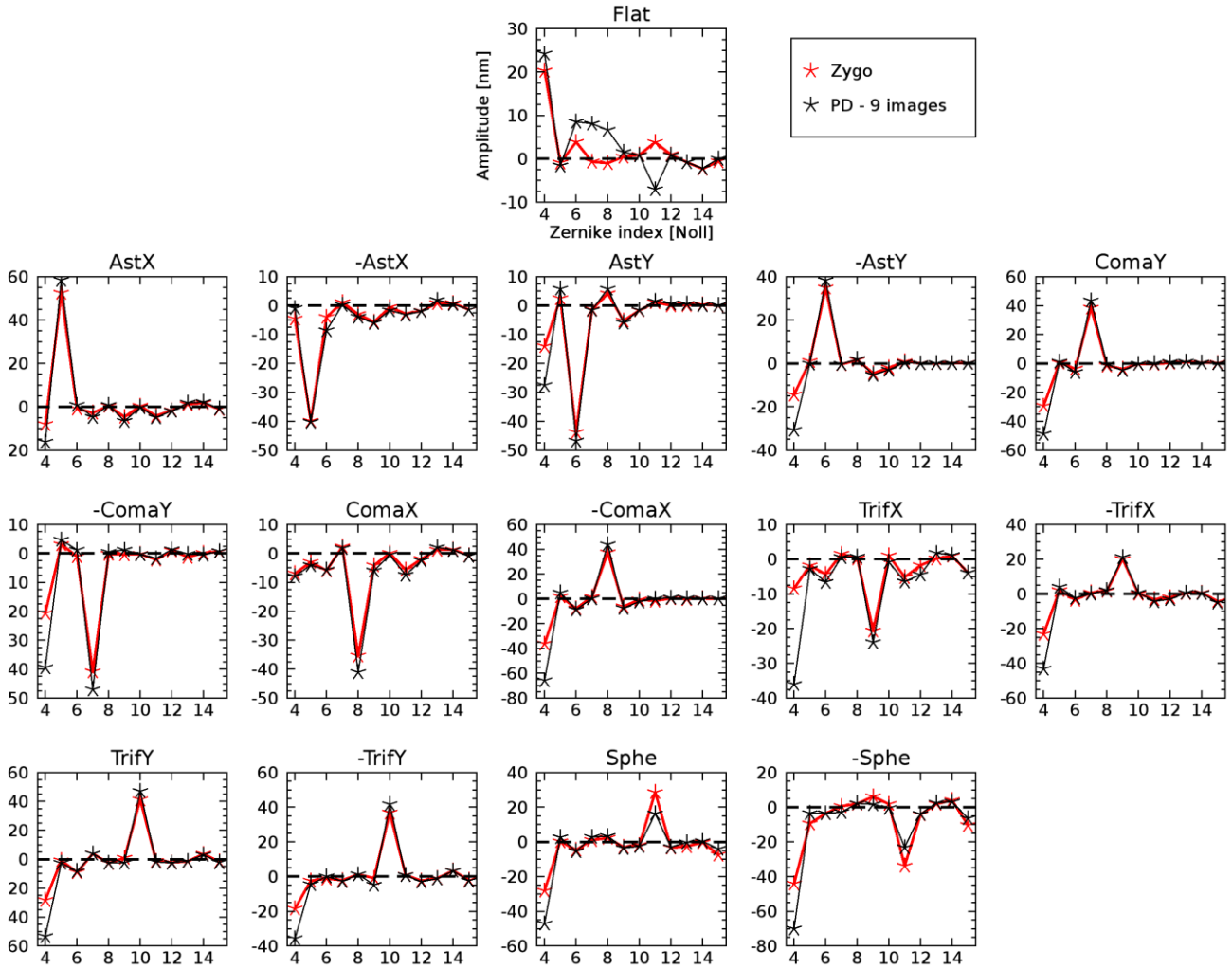

Figure 15 Comparison between Zygo measurements and PD reconstructions using the whole set of 9 images, for the single modes injected with the DL.

5. CONCLUSIONS

We used a previously characterized deformable lens to introduce known aberrations in an optical path. Using more images intra- and extra-focus, corresponding to a maximum of 2.5 waves in defocus, we used the Phase Diversity to reconstruct aberrations without wavefront sensor. This technique is used for sensing non-common path aberrations (NCPA) in SHARK-NIR, the new-generation high-contrast imager for the Large Binocular Telescope (LBT). The PD reconstructions match the Zygo measurements, and individual aberrations are well recovered.

REFERENCES

[1] D. Vassallo, J. Farinato, J.-F. Sauvage, T. Fusco, D. Greggio, E. Carolo, V. Viotto, M. Bergomi, L. Marafatto, A. Baruffolo, and M. De Pascale., "Validating the phase diversity approach for sensing NCPA in SHARK-NIR, the second-generation high-contrast imager for the Large Binocular Telescope," presented at Proc.SPIE, 10 July 2018.

[2] Maria Bergomi, J. F., Luca Marafatto, Elena Carolo, Davide Ricci, Daniele Vassallo, Luigi Lessio, Valentina D'Orazi, Davide Greggio, Dino Mesa, Kalyan Kumar Radhakrishnan Santhakumari, Gabriele Umbriaco,

Valentina Viotto, Oscar M. Montoya, Lars Mohr, Andrea Baruffolo, Federico Biondi, Sona Chavan, Marco De Pascale, Paul Grenz, Fulvio Laudisio, Jarron M. Leisenring, Fernando Pedichini, Roberto Piazzesi, Enrico Pinna, Alfio Puglisi, Simonetta Chinellato, Marco Dima, Simone Di Filippo, Roberto Ragazzoni, Andrea Bianco, Alexis Carlotti, Cristina Knapic, Martina Vicinanza, Alessio Zanutta, Julian Christou, Laura Funk., "SHARK-NIR: from design to installation, ready to dive into first light," Proc. of SPIE 12187, "Modeling, Systems Engineering, and Project Management for Astronomy X", edited by George Z. Angeli, Philippe Dierickx, (In Press) (2022).

[3] Luca Marafatto, M. D. P., Elena Carolo, Maria Bergomi, Federico Biondi, Davide Greggio, Fulvio Laudisio, Luigi Lessio, Davide Ricci, Gabriele Umbriaco, Daniele Vassallo, Valentina Viotto, Jacopo Farinato, Kalyan Kumar Radhakrishnan Santhakumari., "SHARK-NIR on its way to LBT," Proc. of SPIE 12184. Society of Photo-Optical Instrumentation Engineers (SPIE) Conference Series (2022).

[4] Jacopo Farinato, F. R., Andrea Baruffolo, Maria Bergomi, Andrea Bianco, Federico Biondi, Elena Carolo, Alexis Carlotti, Sona Chavan, Simonetta Chinellato, Marco De Pascale, Marco Dima, Valentina D'Orazi, Steve Ertel, Davide Greggio, Thomas Henning, Fulvio Laudisio, Luigi Lessio, Demetrio Magrin, Luca Marafatto, Dino Mesa, Lars Mohr, Manny Montoya, Kalyan Radhakrishnan, Davide Ricci, Gabriele Umbriaco, Daniele Vassallo, Valentina Viotto, Alessio Zanutta, Simone Antoniucci, Carmelo Arcidiacono, Francesca Bacciotti, Pierre Baudoz, Angela Bongiorno, Laird Close, Simone Di Filippo, Simone Esposito, Paul Grenz, Olivier Guyon, Jarron M. Leisenring, Fernando Pedichini, Roberto Piazzesi, Enrico Pinna, Elisa Portaluri, Alfio Puglisi, Roberto Ragazzoni., "SHARK-NIR, ready to 'swim' in the LBT northern hemisphere 'ocean,'" Proc. of SPIE 12185, "Adaptive Optics Systems VIII", edited by Laura Schreiber, Dirk Schmidt, Elise Vernet, (In Press) (2022).

[5] Daniele Vassallo, T. F., Maria Bergomi, Elena Carolo, Davide Greggio, Luca Marafatto, Gabriele Umbriaco, Jacopo Farinato, Andrea Baruffolo, Kalyan Kumar Radhakrishnan Santhakumari, Valentina Viotto, Jean-François Sauvage., "Laboratory demonstration of focal plane wavefront sensing using phase diversity: a way to tackle the problem of NCPA in SHARK-NIR. Part II: New characterization tests and alternative wavefront sensing strategies," Proc. of SPIE 12185, "Adaptive Optics Systems VIII", edited by Laura Schreiber, Dirk Schmidt, Elise Vernet, (In Press) (2022).

[6] Bonora, S., Jian, Y., Zhang, P., Zam, A., Pugh, E. N., Zawadzki, R. J. and Sarunic, M. V., "Wavefront correction and high-resolution in vivo OCT imaging with an objective integrated multi-actuator adaptive lens," Opt. Express **23**(17), 21931–21941 (2015).

[7] Martino Quintavalla, Mattia Spagnol, Lyu Abe, Marcel Carbillet, Eric Aristidi, Jacopo Mocci, Riccardo Muradore, and Stefano Bonora., "XSAO: an extremely small adaptive optics module for small-aperture telescopes with multiactuator adaptive lens," Journal of Astronomical Telescopes, Instruments, and Systems **6**(2), 1–20 (2020).

[8] Quintavalla, M., Bergomi, M., Magrin, D., Bonora, S. and Ragazzoni, R., "Correction of non-common path aberrations in pyramid wavefront sensors to recover the optimal magnitude gain using a deformable lens," Appl. Opt. **59**(17), 5151–5157 (2020).

[9] Umbriaco, G., Carolo, E., Vassallo, D., Greggio, D., Marafatto, L., Farinato, J., Baudoz, P., Bergomi, M., Biondi, F., Lessio, L., Carlotti, A., Ragazzoni, R. and Viotto, V., "The optical alignment of the coronagraphic masks of SHARK-NIR: paving the way for exoplanets detection and characterization," Society of Photo-Optical Instrumentation Engineers (SPIE) Conference Series **11447**, 114474R (2020).

[10] Robert A. Gonsalves., "Phase diversity: math, methods and prospects, including sequential diversity imaging," presented at Proc.SPIE, 24 May 2018.